Construction and Building Materials 220 (2019) 177–186

Contents lists available at ScienceDirect

Construction and Building Materials

journal homepage: www.elsevier.com/locate/conbuildmat

Ultra-high strength cement-based composites designed with aluminum oxide nano-fibers

Scott Muzenski [a,*], Ismael Flores-Vivian [b], Konstantin Sobolev [c]

[a] Rao Research and Consulting, LLC, McLean, VA, United States
[b] Universidad Autonoma de Nuevo León, Nuevo León, Mexico
[c] Department of Civil and Environmental Engineering, University of Wisconsin-Milwaukee, Milwaukee, WI, USA

HIGHLIGHTS

- Use of Al_2O_3 nanofibers can boost the strength of cement-based materials to 195 MPa.
- Nano-fibers can provide the CSH nano-reinforcement and reduction of shrinkage.
- In UHPC, the incorporation of Al_2O_3 nanofibers can replace silica fume or metakaolin.

ARTICLE INFO

Article history:
Received 23 January 2019
Received in revised form 21 May 2019
Accepted 28 May 2019
Available online 8 June 2019

Keywords:
Nano-alumina
Nanofibers
Ultra-high strength
Oil well cement
Metakaolin
Silica fume

ABSTRACT

The use of nanomaterials has become a popular way to improve the performance of cement-based composites. At the same time, ultra-high strength concrete is becoming more widely used. These materials provide superior durability to infrastructure elements, reducing the need for maintenance or early replacement. The performance boost is achieved by producing a denser microstructure and, in the case when nanofibers are used, may reduce the initiation of cracks. Aluminum oxide nanomaterials have the potential to provide a significant increase in compressive strength of cement-based materials. Here, the effect of incorporation of aluminum oxide nanofibers in oil well cement based mortars and composites is reported. The design of ultra-high strength concrete often requires a precisely tuned aggregate gradation, the use of specific cement types and high quantities of silica fume and superplasticizers along with high temperature and curing under elevated pressure. It was demonstrated that the use of small quantities of aluminum oxide nanofibers in an oil well cement based mortar could provide a compressive strength approaching 200 MPa. These levels were achieved at a considerably lower dosage of silica fume. It is envisioned that the high strength matrix is formed due to the reinforcing of calcium silicate hydrate layers which are formed around the nanofibers. This research demonstrated that due to a "shish kebab" effect the addition of well-dispersed aluminum oxide nanofibers at a very small dosage of 0.25% (by mass of cement) could provide up to 30% increase in compressive strength of cementitious systems, helping to meet the benchmarks for ultra-high strength cement-based composites.

1. Introduction

Ultra-high strength cement-based composite (UHSCC) materials, including ultra-high-performance fiber reinforced concrete (UHPC), are becoming a popular solution in modern construction practice [1–5]. These new composite materials tend to provide superior durability and allow thinner structural sections to be used. However, the use of ultra-fine fillers and high quantities of reactive silica materials results in a significant increase in cost compared to conventional concrete. If a cement-based material with similar properties was developed without the need for such high volumes of sub-micron sized and ultra-fine components, the difference in price with conventional concrete could be significantly reduced.

The properties of cementitious matrices are often considered as one of the most important features contributing to the performance of the composite. These properties are of even greater importance when ultra-high strength cement-based materials are considered. The water to binder ratio is one of the critical parameters in the design of high strength and ultra-high strength

* Corresponding author at: 1775 Tysons Blvd., 5th Floor, Tysons, VA 22102, United States.
E-mail address: swm@uwmalumni.com (S. Muzenski).

https://doi.org/10.1016/j.conbuildmat.2019.05.175
0950-0618/

composites, as very low water to binder ratio is required to achieve higher strength. It was reported that the water to binder ratio in UHPC could be as low as 0.15 [1–3]; however, the required strength of 150 MPa was achieved with water to binder ratios of 0.25 or less [4–6].

The type of a binder, reactive powder component (RPC), and type of supplementary cementitious materials are of key importance when designing ultra-high strength cement-based materials. Silica fume is often a critical ingredient used as an RPC. Silica fume is also an ultra-fine supplementary cementitious material with an average particle diameter less than 1 μm and larger specific surface area; therefore, it can occupy the void space (interfacial transition zone) between the cement grains and also between the aggregates and paste. This, in turn, results in a better bond between the paste and the aggregates, which is often a limiting factor in the strength of composites. In ultra-high strength cement-based materials, silica fume is often used at 10% to 30% by mass of cement [7,8], but is often considered at an optimal dosage of 25% [4,9].

An alternative to high quantities of silica fume is the use of a relatively low dosage of nano-particles. Nano-particles can often be just as effective as micro-particles but at significantly reduced quantities because of their higher surface area to volume ratio [10]. For this reason, the use of nanoparticles in cement-based composites has gained considerable attention in recent years. Benefits related to strength, modulus of elasticity, rheological properties, as well as other performance characteristics, have been observed. However, the use of nano-alumina (nano-Al_2O_3) has not had much attention for application in cement-based materials. The reported work used nano alumina particles, as opposed to aluminum oxide nanofibers. Here, the nano-aluminum oxide particles, much like any nanomaterial, enabled the reduction in porosity of cement-based composites by providing a denser interfacial transition zone [11]. However, the use of these nanomaterials, especially at volumes of up to 7%, were found to provide little to no improvement in compressive strength and was also found to reduce the workability [12]. In the same study, the use of the optimal volume of 1% nano-alumina was found only slightly to increase the compressive strength of a cement-based material. The nanomaterials may also be capable of reducing the amount of chloride diffusion and penetration; however, not to the same extent as nanosilica or nano-clays [13]. Currently, there has been no work reported on the use of Al_2O_3 nanofibers in cementitious composites. However, these new products have been used in other industries for improving the ductility of ceramics, super-fine abrasives, engineered plastics, fiber reinforced composites, and polymer-based coatings. Despite no experience on the use of the Al_2O_3 nanofiber material, there still can be a great potential for their application in cement-based materials.

Although aluminum oxide nanomaterials have rarely been used in cement-based materials, one may hypothesize that Al_2O_3 nanofibers can contribute to performance in similar ways as other nanomaterials by providing a seeding effect and acting as a nano-reinforcement (“shish kebab” effect). Here, one of the more common nanomaterials used in cement-based materials is nanosilica. It has been found to accelerate cement hydration by the formation of calcium-silicate-hydrate (CSH) and the dissolution of tricalcium silicates (C_3S) [14]. The acceleration can also be attributed to the nanosilica acting as a seed for the nucleation of CSH [15]. It has been observed that the use of nanosilica in cementitious materials can generate a denser packing of hydration products, a refinement of the pore structure, and an improved interfacial transition zone [16–19]. It is not expected that nano-aluminum oxide would have the same effects as nanosilica; however, similar interactions may occur at the nano level.

The reported research on carbon nanofibers or carbon nanotubes (CNT) may provide some indication of how the Al_2O_3 nanofibers would behave from a mechanical standpoint. The carbon nanomaterials have been found to accelerate the hydration of cement-based materials by acting as nucleation sites for the formation of CSH [20–22]. Additionally, up to 45% increase in compressive strength [22] and an increase in flexural strength have been reported [23]. This was explained by the CNT ability to reinforce the composite and also to potentially reduce the amount of fine pores within the cementitious composite resulting in a lower capillary void space [24,25].

Based on the reported abilities of nanoparticles to provide superior performance to cement-based materials, it is hypothesized the addition of Al_2O_3 nanofibers should result in improved performance. Specifically, the aluminum oxide nanofibers could act as a nucleation site for the formation of hydration products, as well as providing nanoscale reinforcement for CSH, restraining the swelling and shrinkage deformations and ultimately the formation of micro-cracks and thus improving the strength.

This research aims to test the hypothesis that the addition of Al_2O_3 nanofibers will increase the compressive strength of cement-based materials by acting as a nucleation site for the formation of hydration products and providing a reinforcing effect within the CSH. Compressive strength tests, chemical shrinkage, monitoring of heat release during hydration, and observing diluted samples through scanning electron microscopy were performed to evaluate if this hypothesis is correct.

2. Experimental procedures

2.1. Materials

Type H oil well cement meeting the requirements of ASTM C150 [26] for Type V Portland cement was used as the main cementitious material. The chemical composition of Type H cement was 21.8% SiO_2, 3.1% Al_2O_3, 4.5% Fe_2O_3, 64.3% CaO, 2.7% MgO, 1.6% SO_3, 0.2% Na_2O, and 0.2% K_2O as determined by X-Ray Fluorescence (XRF) technique. The potential phase compositions were then 69.1% C_3S, 10.4% C_2S, 13.1% C_4AF, 0.5% C_3A, and 0.17% Na_2O_{equi}. Supplementary cementitious materials (SCM) were also used which included silica fume and metakaolin. Silica fume was represented by spherical particles with sizes between 0.1 and 1 μm. Metakaolin was represented by rough and flaky microparticles with larger sizes from 0.8 to 12 μm.

Chemical admixture used in this research included high range water reducing (superplasticizing) admixture (HRWRA) which was used for the dispersion of Al_2O_3 nanofibers. The HRWRA was a commercially available polycarboxylate (PCE) superplasticizer (SP) with a 31% solid concentration. The Al_2O_3 nanofibers used in this research were synthesized from liquid phase aluminum and then grown to the lengths of 50 mm. These fibers are crystalline γ-alumina with a surface area of 155 m^2/g. The single crystal tensile strength of the fiber is 12 GPa while the modulus is 400 GPa. The typical fiber diameter was 10–20 nm, and the fibers are commonly shipped in tablets (Fig. 1). Upon dispersion, the fibers maintain their diameter but break down to lengths between 10 and 65 μm depending on the dispersion technique.

The Al_2O_3 nanofibers were dispersed by placing a full tablet (puck) of nanofibers (typically between 35 and 45 g) in a plastic container. A solution of de-ionized water with SP was then added to the container. These materials were blended by the mass so that that dispersion was composed of 1.45% SP (by solids), 3.85% Al_2O_3 nanofibers, and 94.7% distilled water. The solution with the nanofibers was then hand mixed for 3 to 5 min using a stirring rod to break up any large agglomerates of fiber. The dispersion was then dispersed using a high-speed mixer (HSM) at 8,000 rpm in combination with a 20 kHz ultrasound treatment at an amplitude of 85%

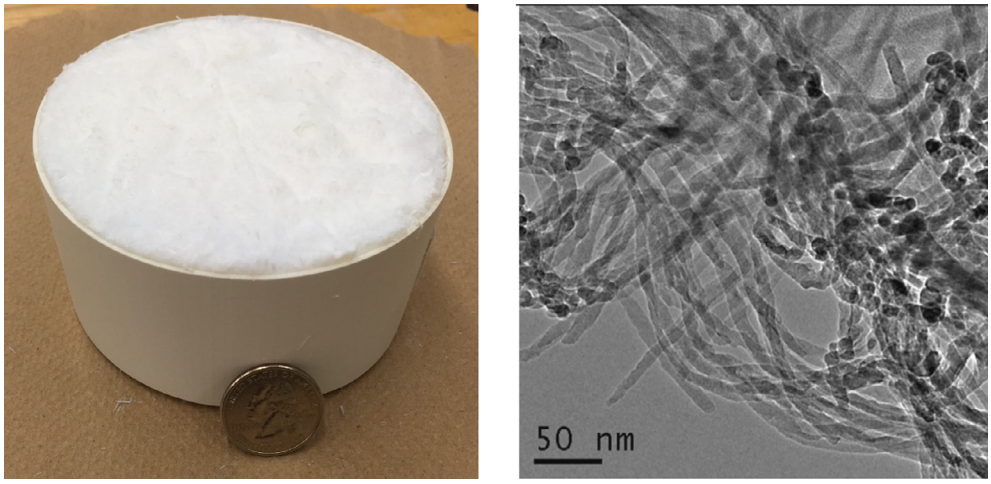

Fig. 1. The puck of Al_2O_3 nanofibers prior to dispersion (left) and transmission electron microscope image of Al_2O_3 nanofibers after dispersion (right, courtesy of AFN technologies).

(21.5 μm). Water and ice were used on the exterior of the container to keep the temperature of the blend below 50 °C. The water and ice were replaced regularly throughout the dispersion process. The dispersion was then left to disperse the product for 1 or 3 h.

Special precautions were taken when handling the nanofibers for the dispersions. These materials are extremely small and light; therefore, are prone to become airborne. These materials can also be potentially hazardous. To meet the safety requirements, the nanomaterials were weighed and added to the liquid phase (the same liquid used for the admixtures or dispersions) in a glove box to assure no airborne particles.

Standard graded silica sand conforming to ASTM C778 [27] was used for mortar preparation. This sand is graded so that the majority (96%) of the aggregate particles falls between the No. 30 and No. 100 sieves, Fig. 2.

2.2. Experimental design

The addition of the nanofibers could contribute to the compressive strength in several different ways. First, the nanofibers could be acting as a viscosity-modifying admixture, allowing additional quantities of PCE superplasticizers to be used without the risk of segregation and, in turn, resulting in better dispersion and a denser cementitious matrix. Next, the nanofibers could be acting as seeds to promote the formation of hydration products along the fibers. This would result in hydration products forming around the fibers which would act as reinforcement bars for the CSH. This would also provide a stiffer cementitious matrix that would improve the material's resistance to the formation of micro-cracks as well as drying and swelling deformations. Another explanation for the strength enhancement could be that the ultra-sonification of the SP portion used with nanofibers may change the structure resulting in the enhancement of its performance.

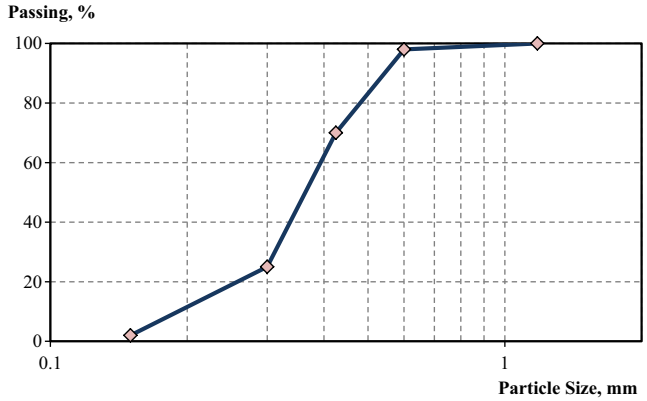

Fig. 2. The gradation of standard silica sand.

This research program included a series of experiments on mortars and cement pastes in determining the effects of Al_2O_3 nanofibers on cement-based materials and the pathway for the most efficient use. First, cement pastes were investigated to determine the underlying effects of Al_2O_3 nanofibers. Mortars were then tested to determine the optimal nanofiber dispersion method, dosage of nanofibers, and the effect of supplementary cementitious materials (SCM) for maximum strength. The complete set of compositions used by the experiment program is defined in Table 1. All mixes used a W/CM of 0.173 and all mortars used an S/CM of 0.50. The only difference between the pastes and mortars was that some additional SP was used for the dispersion of nanofibers in the mortar (0.10% in the mortar and an additional amount used for the dispersion) whereas, in pastes, 0.04% was used in the dispersion and 0.06% in the mix totaling 0.10%. This approach was considered to better understand the effects of nanofibers and help to detect if the structure of the PCE is being altered during the ultrasonification.

Additionally, the experimental matrix for these tests was designed so that the benefits of both silica fume (or metakaolin) and Al_2O_3 nanofibers can be evaluated. Therefore, based on this study, the major contributors (addition of silica fume, metakaolin, Al_2O_3 nanofibers, or a combination) to improved performance were expected to be determined.

The dosages of nanofibers used in this research were relatively small, but nanomaterials are expected to be effective at small quantities [25]. Here, the maximum nanofiber content was 0.5% (by weight) of the cementitious material. This dosage was specified because a considerable volume of water is required for the dispersion of nanofibers (which counts towards the W/CM) and any additional quantities of nanofibers would result in a water demand more considerable than that to maintain the same, relatively low W/CM. In addition to varying quantities, the fibers that had been dispersed for 1 and 3 h were tested.

Some mixtures were designed to determine the effects of supplementary cementitious materials in binders with Al_2O_3 nanofibers. This experiment was used to determine if small quantities

Table 1
Experimental Program for Cement Pastes and Mortars with Al_2O_3 Nanofibers.

Research Phases	Mix ID	SP, % of CM	SF, % of CM	MK, % of CM	Al_2O_3, % of CM	Nano-Fiber Dispersion Time, hours
Portland Cement (PC) Pastes	PR0-0-0	0.1	0	0	0	N/A
	PR0-25-3	0.1*	0	0	0.25	3
	PS1-0-0	0.1	1	0	0	N/A
	PS1-25-3	0.1	1	0	0.25	3
Effect of Nano-Fiber Quantity and Dispersion Time in PC-SF Mortars	MS1-0-0	0.1	1	0	0	N/A
	MS1-10-1	0.1	1	0	0.1	1
	MS1-25-1	0.1	1	0	0.25	1
	MS1-50-1	0.1	1	0	0.5	1
	MS1-10-3	0.1	1	0	0.1	3
	MS1-25-3	0.1	1	0	0.25	3
	MS1-50-3	0.1	1	0	0.5	3
Effect of Supplementary Cementitious Materials in PC-SF-MK Mortars	MR0-0-0	0.1	0	0	0	N/A
	MR0-25-3	0.1	0	0	0.25	3
	MK1-0-0	0.1	0	1	0	N/A
	MK1-25-3	0.1	0	1	0.25	3
	MK5-0-0	0.1	0	5	0	N/A
	MK5-25-3	0.1	0	5	0.25	3
	MK10-0-0	0.1	0	10	0	N/A
	MK10-25-3	0.1	0	10	0.25	3
	MS1-0-0	0.1	1	0	0	N/A
	MS1-25-3	0.1	1	0	0.25	3
	MS5-0-0	0.1	5	0	0	N/A
	MS5-25-3	0.1	5	0	0.25	3
	MS10-0-0	0.1	10	0	0	N/A
	MS10-25-3	0.1	10	0	0.25	3

* The SP content in cement pastes corresponds to the total content including SP in the mix and SP in the dispersion.

of nanofibers can provide the same, if not improved, compressive strength compared to relatively high quantities of silica fume and metakaolin commonly used in UHPC formulations. Additionally, larger quantities of micro-particles combined with nanofibers were tested for a synergetic increase in strength. It should be noted that the composition with 10% metakaolin but without nanofibers (MS10-0-0) was unmixable at a very low W/CM of 0.173 as the use of a high quantity of metakaolin resulted in a mix with unusably low workability. However, the same mix with the addition of nanofibers (MS10-25-3) had adequate workability and was tested.

2.3. Preparation of pastes and mortars

Standard ASTM C305 [28] procedure was used for mixing the mortars and pastes. The dispersion of Al_2O_3 nanofibers was added to the mix as a part of the mixing water. Diluted cement pastes for scanning electron microscope analysis were prepared in small high-density polyethylene (HDPE) containers and mixed by hand for 1–2 min.

Cement pastes or mortars that were used for the isothermal calorimetry were placed into 20 mL HDPE containers and were immediately inserted in the isothermal calorimeter for evaluation. Sealed pastes for SEM investigation were allowed to cure at room temperature in lab conditions in a diluted state. Finally, pastes for chemical shrinkage were placed in the 20 mL glass containers for immediate evaluation at room temperature (25 °C) conditions.

Fresh mortars were placed into 50.8 mm cube molds, compacted and cured as required for compressive testing. Cube molds were cast and compacted in accordance with ASTM C109 [29]. The molds were covered with glass plates and placed in a curing room at room temperature (20 ± 3 °C) and a relative humidity of no less than 90% as per ASTM C192 [30] standards after they were filled with mortar. The samples were then removed from the molds after 24 h and placed in a lime water bath until the testing age. Cement pastes were prepared for chemical shrinkage tests in accordance with ASTM C1608 [31].

2.4. Testing and evaluation of pastes and mortars

The performance of cement pastes and mortars with Al_2O_3 nanofibers was studied in several ways. One of the first tests performed was the evaluation of cement pastes and mortars for the heat flow due to the hydration. This test was performed by placing 25 g of fresh mortars or 10 g of fresh cement paste into a container and evaluating the heat release at 25 ± 1 °C using an isothermal calorimeter for a minimum of 72 h in accordance with ASTM C1679 [32–35]. The degree of hydration (DOH) at a specific age was estimated by the ratio Q/Q_∞, where Q represents the cumulative heat released in a particular time and Q_∞ = 440.8 J/g represents the theoretical amount of heat that is generated when the cement is completely hydrated. The Q_∞ is calculated by multiplying the theoretical value of each hydrating component (C_3S, C_2S, C_3A, and C_4AF) by the proportion of respective component (as determined by XRF) [33–35].

To monitor the performance of cement pastes, chemical shrinkage (CS) tests were performed in accordance with ASTM C1608 Procedure A (volumetric method) [34,36]. The initial reading was taken exactly 1 h after the paste was mixed (this allows time for the sample to achieve the temperature equilibrium within the water bath). The remaining readings were taken every 30–60 min for the next 8 h and then approximately every 8 h after that. The readings were observed to the nearest 0.0025 mL. The chemical shrinkage over time was then calculated as a function of absorbed water over the mass of cement. The cement hydration model proposed by NIST [34] was fitted to the heat of hydration and shrinkage response. The CS_∞ = 0.0532 mL/g represents the theoretical CS that is generated when Portland cement is completely hydrated [34].

Cement pastes were also observed using scanning electron microscopy (SEM). This was accomplished through preparation of diluted samples by mixing slurries of Al_2O_3 nanofibers with cement at a 1:1 ratio. The diluted samples were placed in droplets on a glass slide and allowed to hydrate for 24 h at which time the hydration was halted by placing the sample in alcohol and, after, heating in an oven at 85 °C for 30 min. The samples were then

observed using SEM to determine the structure of hydration products and orientation of nanofibers.

Another test used to monitor the performance of mortars was determining the compressive strength of the samples. This was performed on 50.8 mm cubes in accordance with ASTM C109 [29]. These specimens were tested using an automatic compression machine by loading at a rate of 1.4 kN/s. The maximum load was then recorded and used to calculate the compressive strength of the composite.

3. Results and discussion

3.1. Investigation of cement pastes

3.1.1. Heat of hydration

The heat of hydration profiles of investigated cement pastes are reported in Fig. 3. The identical quantities of PCE superplasticizer were used in all compositions; however, the quantities added during the mixing of pastes was different as some portion of admixture was used for nanofiber dispersion. This approach was used in order to effectively disperse and incorporate the nanofibers. It is envisioned that during the ultrasonication the original structure of PCE is modified and so overall response of the pastes can be different (delayed hydration with the use of ultrasonicated PCE) [33]. Here, in contrast, the use of only 1% silica fume provides a significant increase in the peak heat flow. There is also an acceleration of hydration for compositions with silica fume.

On the other hand, the addition of Al_2O_3 nanofibers resulted in an extension of dormant period. The expectation was that the addition of Al_2O_3 nanofibers would lead to an acceleration of hydration because of the increased surface area and potential seeding effect of the nanofibers; however, this was not the case. The observed response is an indication that the chemical structure of PCE was altered during the ultrasonication similar to the response reported by [17,35,37]. Here, the reactivity of Al_2O_3 material used alone at a very small dosage cannot be contributing to the delay as it is supposed to be a chemically inert material, and increased surface area would likely result in a faster hydration. In spite of initial delay, the addition of nanofibers did result in an increased peak heat flow compared to the reference; yet, not to the same extent observed for silica fume compositions.

The combination of silica fume and nanofibers results in an acceleration of hydration compared to the mix with only nanofibers and a slight decrease in peak heat flow. The heat flow from the combination of silica fume and nanofibers is interesting because one would expect that since both silica fume and nanofibers alone resulted in increased peak heat flow, the combination would result in an even higher peak heat flow. Despite this, the cumulative heat values for two samples with Al_2O_3 nanofibers were the same, indicating that after 40 h these had a similar overall degree of hydration (which was lower than the sample with silica fume alone). This response was only analyzed for the first 40 h; however, available data indicate that the nanofibers are providing some seeding, but this phenomenon may not be the only reason for the potential improvement of compressive strength. The degree of hydration can be correlated to the cumulative heat of hydration using Q_∞ [33,34] which results in 40% of hydration over tested period of 40 h. For reference cement, the heat of hydration over longer periods of time can be estimated from chemical shrinkage data based on the model proposed by NIST [34]. For example, after 170 h, the degree of hydration of 50% and corresponding heat of 224 J/g can be estimated.

3.1.2. Chemical shrinkage

The chemical shrinkage of the same set of cement pastes was tested up to 7-day age. The results of these tests are reported in Fig. 4. The results demonstrate that there is a difference in the response of all tested mixtures. The research results prove that, at the same W/CM ratio, both silica fume and nanofibers generate less chemical shrinkage than the reference sample. The addition of silica fume is generating a denser CSH structure which restricts the volumetric deformations of the sample. The addition of nanofibers to the composite matrix provides even further reduced chemical shrinkage. This is an interesting finding because the chemical shrinkage is correlated with the degree of hydration of a cement-based material [34,36]. The relationship describing the chemical shrinkage and hydration degree was described in [34]; furthermore, the CS data can be correlated with the results from the cumulative heat.

Based on the observations, it may be concluded that nanofibers can provide a reinforcing effect stitching the CSH (i.e., "shish kebab" effect) which can be the reason for reduced shrinkage. This phenomenon may also be a reason for the increased compressive strength expected and observed with the addition of nanofibers. Even though the use of only 1% silica fume on its own provides a denser structure resulting in a low chemical shrinkage, the

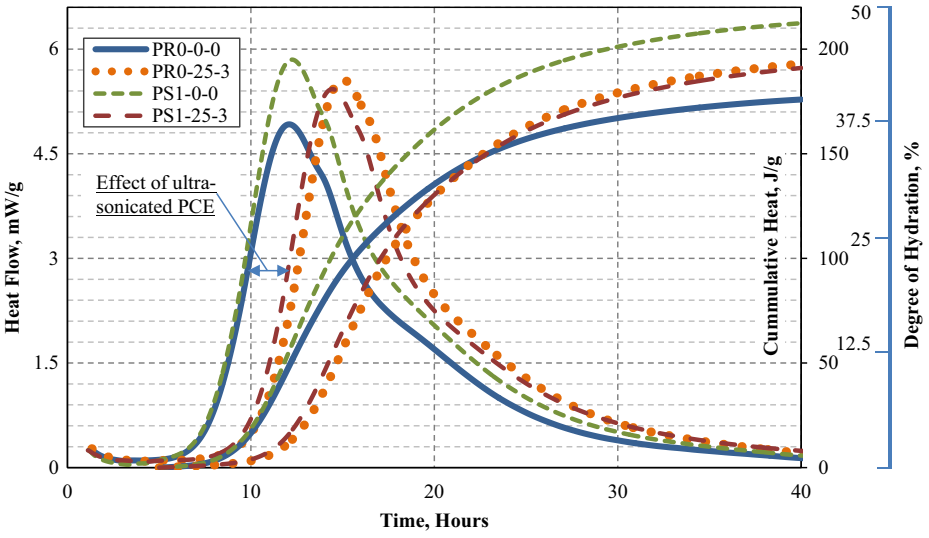

Fig. 3. Heat of hydration of cement pastes with silica fume and Al_2O_3 nanofibers.

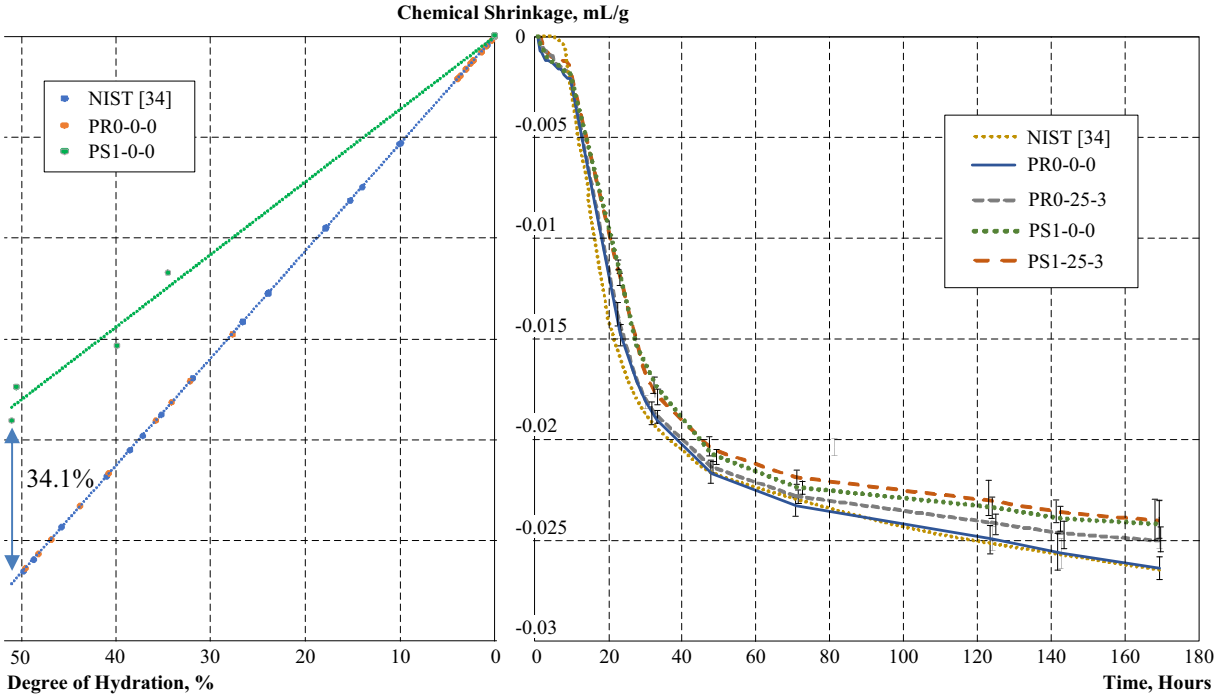

Fig. 4. Chemical shrinkage of cement pastes with Al_2O_3 nanofibers with time (right) and vs. estimated degree of hydration (left).

combination of 1% silica fume with nanofibers did not provide much of an improvement compared to the sample with only nanofibers. These results may indicate that the nanofibers are the main contributor to the reduced chemical shrinkage (and potentially, the compressive strength) while the incorporation of 1% silica fume can provide the densification of the matrix required for the effective anchorage of the nanofibers.

The chemical shrinkage can be modelled as a function of estimated degree of hydration using the approach reported in [34], as explained by Fig. 4. Here, based on the 40-hour heat of hydration and CS data, it was estimated that 40% degree of hydration is reached by the reference cement. The CS of sample with Al_2O_3 nanofibers was standardized to the time in which the same degree of hydration was observed and presented as a function of the degree of hydration. Based on these results, at 50% degree of hydration, the use of nanofibers provides considerable, 34.1% reduction of chemical shrinkage when compared to the reference. This may be an indication that the nanofibers are providing a denser fiber-stitched structure ("shish kebab" effect) that restrains the shrinkage.

3.1.3. Dispersion of Nano-Fibers

The cement pastes were also observed using a scanning electron microscope to observe the distribution of nanofibers and determine if products of cement hydration are forming around the fibers. Here, cement pastes with large quantities of nanofibers equivalent to the cement content were tested. The same fiber dispersions were used in this experiment, meaning that the amount of water required for dispersion was equal to the amount of water used for the mixing of paste. This equates to a very high W/CM of 25. This test was performed in order to visualize the distribution of nanofibers within the system. The nanofibers in the diluted cement paste can be observed in Fig. 5. It appears as though hydration products are forming around the nanofibers which would support the nucleation site hypothesis. In many areas, fibers can be seen protruding from the hardened cement paste. In typical systems with higher cement contents and non-diluted pastes, these protruding fibers could act as reinforcement between the adjacent CSH globules which would improve the modulus and strength of the composite. With the higher magnification, it appears that fibers are well-distributed within a very dense matrix without visible signs of agglomeration; however, higher magnification may be required to report on fiber–matrix interaction.

3.2. The Al_2O_3 nano-fiber type and dispersion time in PC-SF mortars

3.2.1. Heat of hydration

The heat flow of mortars with different types and quantities of nanofiber was tested next. Based on the heat flow curves (Fig. 6), the difference in hydration between the samples with nanofibers dispersed for 1 h and nanofibers dispersed for 3 h seems to be negligible. The longer dispersion time is assumed to require higher quantities of PCE, as it would absorb on the nanostructures during the dispersion process; however, this idea was not supported by the heat flow study. The samples with nanofibers dispersed for longer periods had very similar performance in respect to a delay in hydration. The peak heat flow of the reference sample was slightly higher than that for the samples with nanofibers. This observation is due to the use of additional PCE originating from the dispersion proportional to the dosage of nanofibers. Also, the differences in peak heat flow between the samples with the same dosage of nanofibers were negligible. Even though it was assumed that the use of an additional PCE admixture might be leading to lower heat flow, the samples with higher quantities of nanofibers had higher quantities of superplasticizer and thus also should have had lower peak heat flows. This was not the case, as only delays with maximum peaks were observed. This may be an indication that the use of an additional SP is not resulting in a decrease of the peak heat flow, but rather the ultra-sonification is changing the properties of PCE resulting in the extension of the dormant period.

A delay in the hydration can be detected with an increasing amount of nanofibers. The proportion of nanofibers to PCE was the same for all dispersions; therefore, higher quantities of

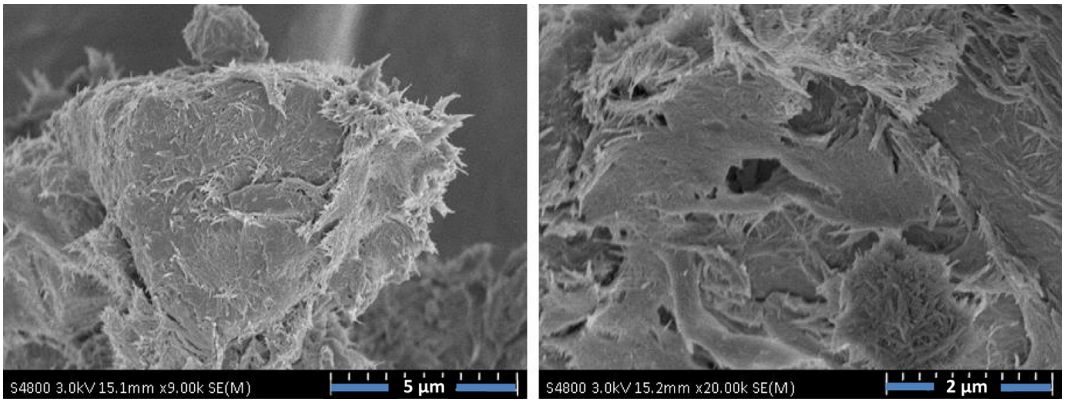

Fig. 5. Scanning electron microscope images of diluted cement pastes with Al_2O_3 nano-fibers at 9,000× magnification (left) and 20,000× magnification (right).

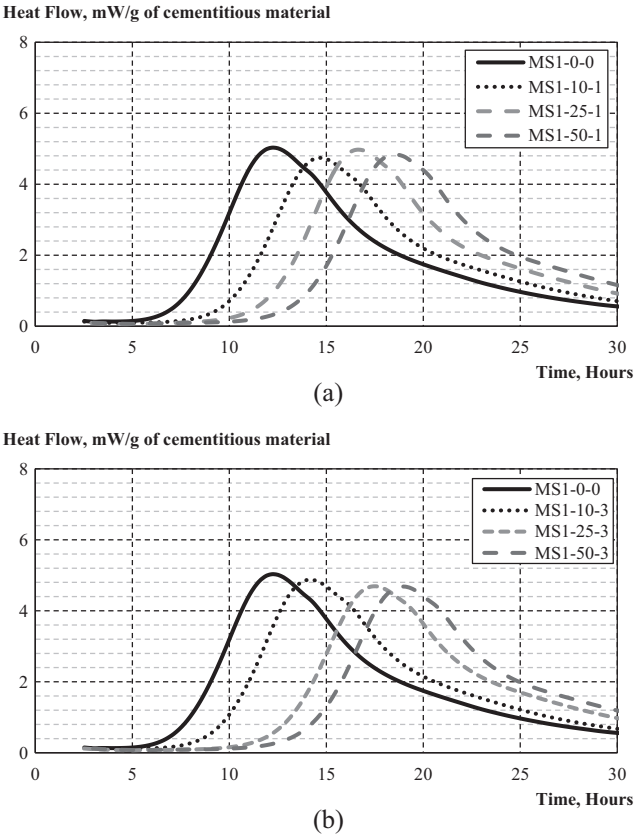

Fig. 6. Heat of hydration of mortars with Al_2O_3 nanofibers dispersed for a) 1 h and b) 3 h.

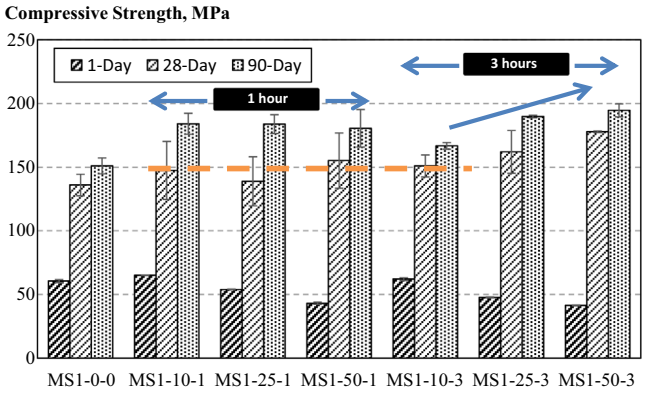

Fig. 7. Compressive strength of mortars with varying quantities of Al_2O_3 nanofibers dispersed for 1 and 3 h.

nanofibers would require the use of higher quantities of SP. With these higher quantities in the system, a larger delay can be expected. Increasing the amounts of SP did not lower the peak heat flow as expected, but did delay the hydration process. This may be an indication that the PCE is attaining the modification of structure and unique properties after ultrasonication.

3.2.2. Compressive strength

The compressive strength of mortars with different quantities of Al_2O_3 nanofibers, as well as nanofibers dispersed for different periods, are reported in Fig. 7. It is clear that the addition of Al_2O_3 nanofibers provides a significant improvement in compressive strength. The best performing sample provided a 29% increase in 90-day strength compared to the reference. When comparing different quantities of nanofibers dispersed for 1 h, there seems to be no trend in compressive strength with all of the values being similar. This may be due to the fact that, at higher dosages, nanofibers can become more agglomerated. This higher degree of agglomeration would make the nanofibers less effective, which could be the reason for little improvement in strength observed with higher quantities. The only trend that can be reported with the nanofibers is that 1-day compressive strength tends to be reduced as higher quantities are used. This is because the higher nanomaterial quantities would absorb some "additional" SP which is consumed and altered during the dispersion. This triggers a delay in hydration as supported by the heat flow curves and thus reduces the early-age compressive strength. However, at later ages (especially, 90 days), it is clear that the addition of higher quantities of nanofibers provides increased compressive strength. Here, the extended dispersion allows for lesser agglomeration and thus enables the fibers to be more effective. The 90-day compressive strength of composites with 0.5% of nanofibers are encouraging demonstrating an increase of 17% compressive strength compared to mixtures with 0.1% of nanofibers. The samples with 0.25% nanofibers had a strength increase of 14% (vs. compositions with 0.1% of nanofibers), which was slightly lower than that for mixtures with 0.50%. This may also indicate that a quantity of 0.25% nanofibers can be considered to be an optimal amount, as doubling the quantity did not provide a significant improvement of strength.

At 90 days, the difference between the samples with nanofibers dispersed for 1 or 3 h is negligible; however, considerable improvement can be observed for the composites hardened for 28 days and

also at an increased dosage of nanofibers. From these results, it may be evident that the higher quantities of well-dispersed nanofibers result in higher compressive strength. Despite the 90-day results of the nanofibers dispersed for 3 h not showing significant improvement compared to those dispersed for 1 h, a longer time may be beneficial to create a more stable dispersion and provide a higher 28-day compressive strength. At 90 days, more complete hydration has occurred so that the benefits of having a better dispersion cannot be detected from the compressive strength data. It is quite possible that a better dispersion is potentially essential to provide improved performance in terms of modulus of elasticity as well as tension and bending properties.

3.3. The effect of supplementary cementitious materials

3.3.1. Heat of hydration

The results from the heat flow curves for samples with different types and quantities of supplementary cementitious materials (Fig. 8) prove that with the addition of small volumes of silica fume or metakaolin, the hydration of Portland cement occurs faster. This may be because the higher surface area of these materials would require larger quantities of PCE-based superplasticizer and thus compensates for the induced delay. In many cases, the samples with metakaolin are hydrating slightly faster than those with silica fume. One reason for this is that metakaolin particles are flaky, requiring higher quantities of superplasticizer for dispersion than the spherical silica fume particles. Additionally, the higher quantity of aluminate phases in metakaolin can speed up the reaction process. There also seems to be a trend that with the higher quantities of silica fume or metakaolin used, there is a lower peak heat flow. This is to be expected as metakaolin and silica fume, or many other supplementary cementitious materials for that matter, are pozzolanic materials that do not produce large quantities of heat during hydration. These materials are siliceous or have aluminous silicate components, and in the presence of water react with calcium hydrates to form the calcium silicate hydrates (CSH). These CSH types are similar to the ones formed from the hydration of C_2S and C_3S; thus these pozzolans demonstrate excellent cementitious properties. The addition of such compounds typically produces slower hydration and increased volume of CSH, resulting in improved strength at later ages. Here, metakaolin and silica fume are very fine particles with high surface areas, which tend to be more reactive than most other pozzolans. This would increase the speed at which these reactions are occurring and, as so, significant improvements in early-age strength may be observed (when the test and performance at a constant W/CM are considered). In many cases, the peak heat release of the samples with metakaolin is higher than the peak heat release of the samples with silica fume. This is because the metakaolin has aluminate phases resulting in the acceleration of hydration and higher heat releases.

When comparing the samples with and without the nanofibers, the hydration process typically occurs at a later stage when the nanofibers are added. This is most likely due to the additional quantities of SP are consumed and altered during the dispersion of the nanofibers. The samples with lower quantities of supplementary cementitious materials often see a more significant delay when nanofibers are present; however, this delay is minor in mixtures with higher volumes of silica fume or metakaolin. This could mean that, at these higher quantities of SCM, much of the superplasticizer is being consumed and no excess is available to delay the hydration. Here, the workability and fluidity are more dependent on the use of metakaolin or silica fume than it is on the use of nanofibers, meaning that the SP used for the dispersion of nanofibers may be necessary when higher quantities of supplementary cementitious materials are used. The samples with nanofibers also tend to have a slightly lower peak heat flows. It would be expected that the addition of nanofibers would result in higher peak heat flows because of additional hydration products being formed at a faster rate, but this was not the case. This is consistent with previous data and may be an indication that the ultra-sonification of the PCE is affecting its properties.

3.3.2. Compressive strength

The compressive strength of samples with varying types and quantities of supplementary cementitious materials is reported in Fig. 9. These samples used 0.25% Al_2O_3 nanofibers (by weight of cementitious materials) as it was determined to be an optimal

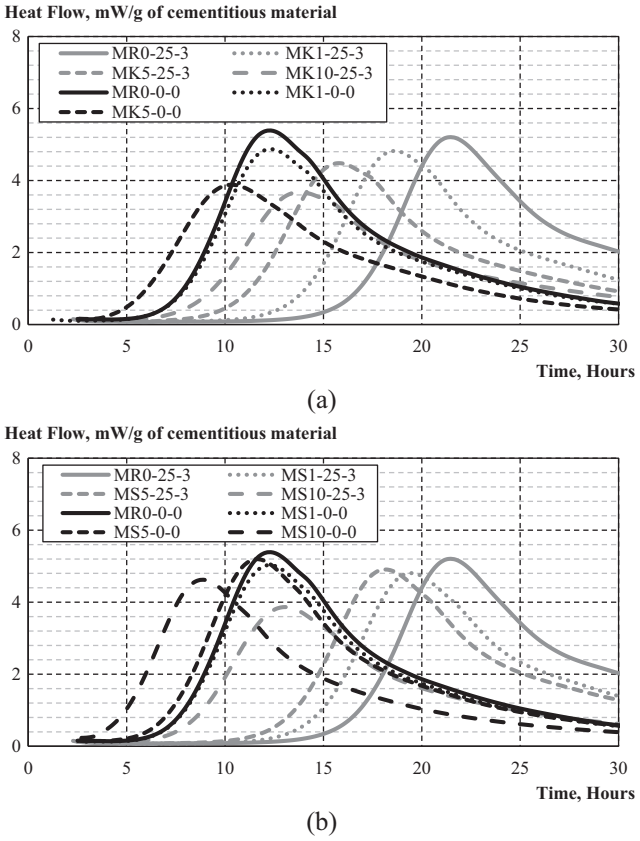

Fig. 8. Heat flow of mortars with Al_2O_3 nanofibers and varying quantities of a) metakaolin and b) silica fume.

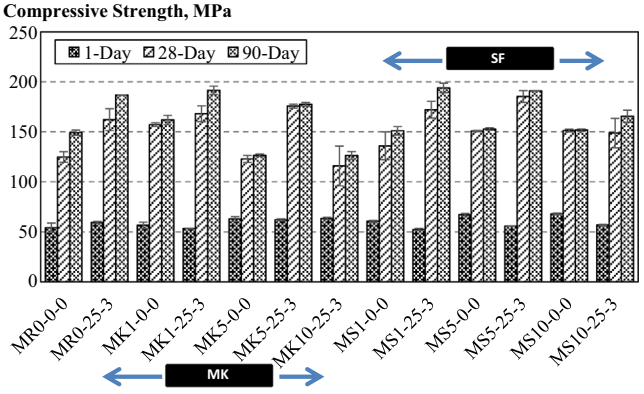

Fig. 9. Compressive strength of mortars with Al_2O_3 nanofibers and varying metakaolin or silica fume.

dosage from the previous study. The samples without nanofibers demonstrated the reductions in compressive strength when larger quantities of SCM were used. This trend was observed for compositions with 5% metakaolin, 5% silica fume, and 10% silica fume. This effect is most likely because these micro-particles were acting as a viscosity-modifying admixture that reduced the workability of the mixtures and generated higher quantities of entrapped air voids. The reduction in compressive strength was more prevalent in the samples with 5% metakaolin than those with 5% or more of silica fume. This can be due to the shape of these micro-particles. The silica fume particles have a spherical shape, whereas the metakaolin particles are more flat and angular, resulting in the reduction of workability defects of the structure and, so, a more significant reduction in compressive strength. These results may also indicate that the current mix design would not be beneficial for the use without the nanofibers.

When comparing samples with Al_2O_3 nanofibers, it is clear that the addition of metakaolin or silica fume improves the compressive strength. For the samples with metakaolin, 1% replacement of cement provides the best strengths, while a reduction in compressive strength was observed at 5% replacement. For the samples with silica fume, 1% and 5% replacement of cement performed the best. When 10% of silica fume was used in combination with Al_2O_3 nanofibers, the compressive strength was reduced because of the additional entrapped air voids and reduced workability. When comparing 1% and 5% silica fume mixtures, the later had approximately an 8% increase in compressive strength at 28 days whereas these two were comparable at 90 days. This allows some flexibility in the material's design. If strength is required at 28 days, 5% silica fume may be beneficial; however, at 90 days the use of only small quantities of silica fume, say 1% but in combination with Al_2O_3 nanofibers, can be beneficial. In many cases, for ultra-high strength cementitious composites, high quantities of silica fume are required to achieve the desired strength. Here, the same desired strength can be obtained with very small quantities of silica fume used in combination with nanofibers.

4. Conclusions

Ultra-high strength cement-based composite (UHSCC) materials are becoming a popular solution in modern construction practice. The strength performance of these materials allows thinner structural sections to be used and, due to an extremely dense cementitious matrix, structures with superior durability can be designed and built. The use of nanoparticles in ultra-high strength cement-based materials is an efficient way to achieve the desired performance with significantly reduced quantities of silica fume (used as a replacement for the main cementitious material). Aluminum oxide nanofibers have yet to be used in cement-based materials at an industrial scale; however, this product has great promise for a measurable boost in compressive strength.

This work demonstrated that ultra-high strength cement-based materials can be engineered with relatively low quantities of silica fume. The addition of aluminum oxide nanofibers to cement-based mortar at a dosage of 0.25% (by weight of cementitious materials) significantly improves the compressive strength. This approach can provide a boost of compressive strength approaching up to 200 MPa. This is evident by the 30% increase in compressive strength of the composite when compared with strength of material with only 1% of silica fume. Besides, additional quantities of Al_2O_3 nanofibers or higher quantities of supplementary cementitious materials did not significantly improve the performance and, potentially, can have negative effects on the performance of composites produced at a very low W/CM. The use of 1% metakaolin as cement replacement also provided promising results; however, the compressive strength of metakaolin based compositions was slightly lower than that of materials with 1% silica fume.

The adequate dispersion of the nanofibers is also critical to achieve the top performance. A longer dispersion time should result in lesser agglomeration of fibers and thus can allow the boost of performance. Even though the compressive strength tests did not indicate a considerable difference in the 90-day compressive strength between the compositions with nanofibers dispersed for 1- or 3 h, the 28-day compressive strength was better for samples with nanofibers dispersed for 3 h. It was also observed that the longer dispersion time could result in a more stable dispersion.

It is assumed that the improved behavior expected with the addition of aluminum oxide nanofibers was due to the nanofibers acting as a seed for the formation of hydration products and also providing the reinforcing effect for the CSH formations, reducing the development of micro-cracks. It was demonstrated that the chemical shrinkage of cementitious composites with aluminum oxide nanofibers was reduced by 34.1% vs. reference Portland cement system produced at the same W/CM ratio and dosage of superplasticizer. The proposed performance enhancement theories are based on the results and analysis of heat flow curves, chemical shrinkage data, and microstructure observations; however, more in-depth studies may be required to verify these concepts. Another aspect of this work that may require additional research is to investigate the transformation of the PCE-based superplasticizer during the ultrasonication. Additionally, more research must be performed on the interaction of developed cement-based composite with macro-fibers to produce the family of ultra-high performance fiber-reinforced concrete.

Declaration of Competing Interest

None.

Acknowledgments

The authors would like to thank the University of Wisconsin-Milwaukee Research Growth Initiative (RGI) for the support of Prof. Sobolev's research group. The authors would also like to thank LafargeHolcim, Burgess Optipozz, Handy Chemicals, ANF Technology, and Elkem for the donation of materials. A special thanks are conveyed to Marina Kozhukhova and Behrouz Farahi for their help.

References

[1] B.A. Graybeal, J.L. Hartmann, Strength and durability of ultra-high performance concrete, Concrete Bridge Conference Portland Cement Association, 2003.
[2] B. Aarup, *CRC-a* special fiber reinforced high-performance concrete, International Symposium on Advances in Concrete through Science and Engineering, 2004.
[3] D. Bierwagen, A. Abu-Hawash, Ultra-high performance concrete highway bridge, Proceedings, 2005.
[4] Development of Non-Proprietary Ultra-High Performance Concrete for Use in the Highway Bridge Sector, Techbrief - FHWA Turner-Fairbank Highway Research Center.
[5] B. Graybeal, Construction of field-cast ultra-high performance concrete connections (No. FHWA-HRT-12-038), 2012.
[6] J. Plank et al., Effectiveness of polycarboxylate superplasticizers in ultra-high strength concrete: the importance of PCE compatibility with silica fume, J. Adv. Concr. Technol. 7 (1) (2009) 5–12.
[7] P. Richard et al., Les Bétons de Poudres Réactives (BPR) à ultra haute résistance (200 à 800 MPa), Annales de l'institut technique du bâtiment et des travaux publics, 1995.
[8] G. Long, X. Wang, Y. Xie, Very-high-performance concrete with ultrafine powders, Cem. Concr. Res. 32 (4) (2002) 601–605.
[9] K. Wille et al., Ultra-high performance concrete and fiber reinforced concrete: achieving strength and ductility without heat curing, Mater. Struct. 45 (3) (2012) 309–324.
[10] Florence Sanchez, Konstantin Sobolev, Nanotechnology in concrete–a review, Constr. Build. Mater. 24 (11) (2010) 2060–2071.

[11] Z. Li et al., Investigations on the preparation and mechanical properties of the nano-alumina reinforced cement composite, Mater. Lett. 60 (3) (2006) 356–359.
[12] A. Nazari et al., Influence of Al_2O_3 nanoparticles on the compressive strength and workability of blended concrete, J. Am. Sci. 6 (5) (2010) 6–9.
[13] X. He, X. Shi, Chloride permeability and microstructure of Portland cement mortars incorporating nanomaterials, Transp. Res. Record 2070 (1) (2008) 13–21.
[14] J. Björnström et al., Accelerating effects of colloidal nano-silica for beneficial calcium–silicate–hydrate formation in cement, Chem. Phys. Lett. 392 (1) (2004) 242–248.
[15] W.A. Gutteridge, J.A. Dalziel, Filler cement: the effect of the secondary component on the hydration of Portland cement: Part I. A fine non-hydraulic filler, Cem. Concr. Res. 20 (5) (1990) 778–782.
[16] T. Ji, Preliminary study on the water permeability and microstructure of concrete incorporating nano-SiO 2, Cem. Concr. Res. 35 (10) (2005) 1943–1947.
[17] Ismael Flores-Vivian et al., The use of nanoparticles to improve the performance of concrete, Nano Conference, 2013.
[18] H. Li, H.-G. Xiao, J.-P. Ou, A study on mechanical and pressure-sensitive properties of cement mortar with nanophase materials, Cem. Concr. Res. 34 (3) (2004) 435–438.
[19] B.-W. Jo et al., Characteristics of cement mortar with nano-SiO2 particles, Constr. Build. Mater. 21 (6) (2007) 1351–1355.
[20] T. Kowald, R. Trettin, Improvement of cementitious binders by multi-walled carbon nanotubes, in: Nanotechnology in Construction, Springer, 2009, pp. 261–266.
[21] X. Xiang et al., Carbon nanotubes as a new reinforcement material for modern cement-based binders, NICOM 2: 2nd International Symposium on Nanotechnology in Construction, RILEM Publications SARL, 2006.
[22] J.L. Luo, Z.D. Duan, The dispersivity of multi-walled carbon nanotubes (NMWTs) and pressure-sensitive property of NMWTs reinforced cement composite, Adv. Mater. Res. 60 (2009) 475–479.
[23] M.S. Konsta-Gdoutos, Z.S. Metaxa, S.P. Shah, Highly dispersed carbon nanotube reinforced cement-based materials, Cem. Concr. Res. 40 (7) (2010) 1052–1059.
[24] M.S. Konsta-Gdoutos, Z.S. Metaxa, S.P. Shah, Multi-scale mechanical and fracture characteristics and early-age strain capacity of high-performance carbon nanotube/cement nanocomposites, Cem. Concr. Compos. 32 (2) (2010) 110–115.
[25] K. Sobolev, M.F. Gutiérrez, How nanotechnology can change the concrete world, Am. Ceram. Soc. Bull. 84 (10) (2005) 14.
[26] ASTM C150-19a Standard Specification for Portland Cement, ASTM International, West Conshohocken, PA, 2017, www.astm.org.
[27] ASTM C778-17, Standard Specification for Standard Sand, ASTM International, West Conshohocken, PA, 2017, www.astm.org.
[28] ASTM C305-14, Standard Practice for Mechanical Mixing of Hydraulic Cement Pastes and Mortars of Plastic Consistency, ASTM International, West Conshohocken, PA, 2014, www.astm.org.
[29] ASTM C109 / C109M-16a, Standard Test Method for Compressive Strength of Hydraulic Cement Mortars (Using 2-in. or [50-mm] Cube Specimens), ASTM International, West Conshohocken, PA, 2016, www.astm.org.
[30] ASTM C192 / C192M-18, Standard Practice for Making and Curing Concrete Test Specimens in the Laboratory, ASTM International, West Conshohocken, PA, 2018, www.astm.org.
[31] ASTM C1608-17, Standard Test Method for Chemical Shrinkage of Hydraulic Cement Paste, ASTM International, West Conshohocken, PA, 2017, www.astm.org.
[32] ASTM C1679-17, Standard Practice for Measuring Hydration Kinetics of Hydraulic Cementitious Mixtures Using Isothermal Calorimetry, ASTM International, West Conshohocken, PA, 2017, www.astm.org.
[33] K. Sobolev, Z. Lin, Y. Cao, H. Sun, I. Flores-Vivian, T. Rushing, T. Cummins, W.J. Weiss, The influence of mechanical activation by vibro-milling on the early-age hydration and strength development of cement, Cem. Concr. Compos. 71 (2016) 53–62.
[34] X. Pang, D.P. Bentz, C. Meyer, G.P. Funkhouser, R. Darbe, A Comparison study of Portland cement hydration kinetics as measured by chemical shrinkage and isothermal calorimetry, Cem. Concr. Compos. 39 (2013) 23–32.
[35] K. Sobolev, Modern developments related to nanotechnology and nanoengineering of concrete, Front. Struct. Civil Eng. 10 (2) (2016) 131–141.
[36] E.-I. Tazawa, S. Miyazawa, T. Kasai, Chemical shrinkage and autogenous shrinkage of hydrating cement paste, Cem. Concr. Res. 25 (2) (1995) 288–292.
[37] K. Sobolev, Z. Lin, I. Flores-Vivian, R.G.K. Pradoto, Nano-engineered cements with enhanced mechanical performance, J. Am. Ceram. Soc. 99 (2) (2016) 564–572.